Distribution Characteristics of De-icing Shear Stress on Thin Plate with Out-of-Plane Flexural Vibration Mode

MIAO Bo[1], *YUAN Lang*[1], *ZHU Chunling*[2*]

1. College of Aerospace Engineering, Nanjing University of Aeronautics and Astronautics, Nanjing 210016, P. R. China;
2. State Key Laboratory of Mechanics and Control for Aerospace Structures, Nanjing University of Aeronautics and Astronautics, Nanjing 210016, P. R. China

(Received 20 March 2023; revised 27 July 2023; accepted 10 August 2023)

Abstract: Ice protection technology based on the mechanical vibration of piezoelectric actuators is a new lightweight and energy-efficient de-icing method. It is gaining increasing interest for use in aviation to mitigate ice-related hazards. The investigation of mechanical vibration de-icing technology encompasses two primary aspects: interface shear stress induced by mechanical vibration and corresponding vibration modes. Finding proper vibration modes to generate enough interface shear stress for de-icing efficiency improvement is a challenge. The vibration mode of the plate is often described by the values m and n, while m and n are the number of anti-nodes in the transversal axis and longitudinal axis separately. This paper is to investigate the distribution characteristics of de-icing shear stress and related vibration parameters (m and n) under different structural vibration modes, so as to establish the structure mode selection criteria for the detail designing process of the mechanical vibration-based ice protection system (IPS). The relationship between interface shear stress and vibration mode parameters under the single force excitation is established by theoretical analysis and simulation methods. A finite element model (FEM), depicting an aluminum plate with an ice layer attached to its surface, is used to simulate the stress-strain levels of the whole structure. According to the simulation outcomes and experimental verification, the distribution characteristics of de-icing parameters are analyzed. The selection of the initial de-icing modes based on the characteristics of m and n values of the flexural vibration modes is emphasized.

Key words: de-icing method; interface shear stress; vibration mode; distribution characteristics; finite element model; ice protection system (IPS)

CLC number: V244.15 **Document code:** A **Article ID:** 1005-1120(2023)S1-0084-12

0 Introduction

Aviation safety will be threatened when aircraft flying through a cloud containing many supercooled water droplets because of the ice formation on the surface of the wings and inlet lip leading edge of engines. Meanwhile, the weight increment and unbalanced mass distribution caused by irregular ice growth on the airplane also put forward a challenge for safety[1-2]. Different types of anti/de-icing methods were developed to try to overcome this problem and mitigate its negative impact on the whole aircraft industry[3]. Ice protection systems with the operation principles of thermal heating, mechanical vibrations, surface chemical treatments, or air layer ionization, were all researched and included in the above-mentioned anti/de-icing methods. The thermal ice protection method is the most common method to be used in the aviation industry because of its high efficiency and reliability. However, the significant energy consumption and high system weight reduce the feasibility of employing certain aviation equipment, such as unmanned aerial vehicles (UAVs) or other lightweight aircraft with limit-

*Corresponding author, E-mail address: clzhu@nuaa.edu.cn.

How to cite this article: MIAO Bo, YUAN Lang, ZHU Chunling. Distribution characteristics of de-icing shear stress on thin plate with out-of-plane flexural vibration mode[J]. Transactions of Nanjing University of Aeronautics and Astronautics, 2023, 40(S1): 84-95.

http://dx.doi.org/10.16356/j.1005-1120.2023.S1.008

ed energy capacity. Under the development tendency of green aviation with carbon neutrality and low energy demand, some new types of ice protection methods should be explored to fulfill this requirement. The mechanical vibration-based de-icing method utilizing piezoelectric actuators as the excitation source has been paid more attention to because of their lightweight and low-energy consumption development potential[4]. This new type of ice protection method has been researched for potential application potential in UAV ice protection regions.

The mechanical vibration de-icing method with piezoelectric actuators is a de-icing method that uses piezoelectric actuators to motivate the whole de-icing structure to vibrate at one or several specific frequencies. Interface shear stress for de-icing purposes will appeal to the interface between the ice layer and substrate structure. Then, the ice layer will be removed from the structure when the connection between the ice layer and the substrate is destroyed by the interface shear stress. These are the ice protection working principles of this new type of de-icing method. Venna et al.[5] utilized this de-icing method on the leading edge structures to validate its application feasibility and achieved effective ice removal. Ultrasonic actuation by piezoelectric actuators for de-icing on helicopter rotor blades was investigated by Palacios et al. and the ice-removing results for impacting ice were also obtained in the ice wind tunnel[6-7]. Mechanism research about the wave-based method for inducing ice delamination was studied by Kalkowski et al. and the guide wave used for de-icing was generated by piezoelectric actuators[8-9]. Habibi et al.[10] introduced a dual de-icing system for wind turbine blades with high-power ultrasonic guide waves and low-frequency forced vibrations. And the de-icing applications on glass fiber-reinforced composite were also been mentioned in Refs.[11-13]. Budinger et al.[14-16] studied the electromechanical characteristics of this mechanical vibration-based de-icing method and gave the analytical and numerical models for describing ice cracks and delamination phenomenon.

Among the studies exploring the use of piezo-actuators for mechanical vibration de-icing, the interface shear stress is a crucial factor that must be examined for ensuring effective ice removal. Moreover, the detailed structural deformation form will influence the generation of interface shear stress, so as to influence the final de-icing results. It means that the design process of exciting sources and the detailed information of structural vibration modes are not very significant in the de-icing system determination. However, many types of research on vibration-based ice-removing methods and systems focus on the de-icing effect of the whole system. The attention on clear theory and design process of single components received is seldom under these circumstances. Rouset et al.[17] analyzed flexural and extensional resonance modes to check the stress ability for initiating ice fractures/delamination and summarized the criteria of the modes selection for inducing the tensile and shear stress generation. However, the shear stress level at the interface of ice and plate in the low and high frequencies range is not given clearly. This will not meet the requirement to select the target vibration mode according to the mode shape of the structure directly. So uncovering the connection between de-icing shear stress and vibration mode shapes characteristics will be a challenge for the detailed designing process of the ice protection system. According to the results in Ref.[17], the flexural vibration modes have a better de-icing effect[14, 17]. So exploring the distribution characteristics of de-icing shear stress on a specific structure under the flexural vibration modes will be treated as the necessary research content. Meanwhile, for the benefit of mechanism research, a thin plate was selected as the specific structure in the following studies. To guarantee that the vibration mode shapes were easy to analyze, the concentrated force was selected as the exciting source.

This paper is arranged into three main sections. Section 1 is dedicated to the basic theories of mechanical vibration de-icing structures under the excitement of a single concentrated force. The relation-

ship between de-icing shear stress and vibration modes was derived from a theoretical angle. Detailed descriptions of simulation models using finite element analysis software are given in Section 2, and the introductions of experimental de-icing setups implemented in the research process of this paper are also provided. Section 3 is a summary of the main results and discussions. This section proposes research on the distribution characteristics of shear stress on a specific structure under the flexural vibration modes, and the verifications with de-icing tests are highlighted finally.

1 Basic Vibration Theories of Thin Plate

For the thin plate under forced vibration situation, the small deflection displacement response of this thin plate $w(x,y,t)$ can be expressed by the normalized displacement modes of the structure $\phi_n(x,y)$, shown as

$$w(x,y,t)=\sum_{n=1}^{\infty}\phi_n(x,y)q_n(t) \tag{1}$$

where $q_n(t)$ is the generalized coordinates corresponding to the normalized displacement modes $\phi_n(x,y)$, and $\phi_n(x,y)$ satisfies orthogonal conditions of thin plate vibration modes, shown as

$$\iint_G \rho h\phi_i(x,y)\phi_j(x,y)\mathrm{d}x\mathrm{d}y=\begin{cases}M_i & i=j\\ 0 & i\neq j\end{cases}\quad i,j=1,2,\cdots,\infty \tag{2}$$

where ρ is the density of the plate, h the plate thickness, M_i the modal mass of the plate, and G the integral area of the whole thin plate.

For the concentrated excitation force $f(x,y,t)=F(x,y)\mathrm{e}^{\mathrm{i}\omega t}$ acting on the point (x,y) of the thin plate, its generalized force corresponding to the generalized coordinate $q_n(t)$ is

$$F_n(t)=\iint_G \mathrm{e}^{\mathrm{i}\omega t}F(x,y)\phi_n(x,y)\mathrm{d}x\mathrm{d}y \tag{3}$$

So the n-order modal force amplitude is

$$F_n=\iint_G F(x,y)\phi_n(x,y)\mathrm{d}x\mathrm{d}y \tag{4}$$

It is assumed that the effective damping force is proportional to the vibration velocity during the vibration process. Considering the orthogonal condition of the displacement modes $\phi_n(x,y)$, the structural strain energy V, kinetic energy T, and dissipation function D under forced vibration can be expressed as

$$\begin{cases}V=\dfrac{1}{2}\displaystyle\sum_{n=1}^{\infty}M_n\omega_n^2q_n^2(t)\\ T=\dfrac{1}{2}\displaystyle\sum_{n=1}^{\infty}M_n\dot{q}_n^2(t)\\ D=\dfrac{1}{2}\displaystyle\sum_{n=1}^{\infty}C_n\dot{q}_n^2(t)\end{cases} \tag{5}$$

where ω_n is the natural frequency of each order of the thin plate corresponding to the natural vibration modes $\phi_n(x,y)$, M_n and C_n are the mass and damping of the beam with the nth vibration mode separately.

Considering the classic force theory, the dynamic characteristics can be derived in the aspect of energy, which can be written as the Lagrange equation[18-19], shown as

$$\frac{\mathrm{d}}{\mathrm{d}t}\left(\frac{\partial T}{\partial\dot{q}_i}\right)-\frac{\partial T}{\partial\dot{q}_i}+\frac{\partial V}{\partial q_i}+\frac{\partial D}{\partial\dot{q}_i}=0\quad i=1,2,\cdots,\infty \tag{6}$$

So substituting the expression of strain energy, kinetic energy, and dissipation function into the above equation, one can obtain the following expression

$$\boldsymbol{M}\ddot{q}(t)+\boldsymbol{C}\dot{q}(t)+\boldsymbol{K}q(t)=\boldsymbol{F}(t) \tag{7}$$

where $\boldsymbol{M}=[m_{ij}]$ is the generalized mass matrix, $\boldsymbol{C}=[c_{ij}]$ the generalized damping matrix, $\boldsymbol{K}=[k_{ij}]$ the generalized stiffness matrix, and $\boldsymbol{F}$ the generalized modal force column matrix.

Considering the orthogonality conditions of displacement, the differential equations that generalized coordinates $q_n(t)$ should satisfy can be written as

$$M_n\ddot{q}_n+C_n\dot{q}_n+K_nq_n=F_n\mathrm{e}^{\mathrm{i}\omega t} \tag{8}$$

where K_n and F_n are the stiffness and the modal force of the beam with the nth vibration mode separately.

For the concentrated excitation force $F=F_0\mathrm{e}^{\mathrm{i}\omega t}$ acting on the point (x_0,y_0) of the thin plate, its modal force at the nth vibration mode can be shown as $F_n=F_0\phi_n(x_0,y_0)\mathrm{e}^{\mathrm{i}\omega t}$. So the steady-state re-

sponse of the thin plate under this excitation force is

$$w(x,y,t)=\sum_{n=1}^{\infty}\frac{F_0\phi_n(x_0,y_0)\phi_n(x,y)\mathrm{e}^{\mathrm{i}(\omega t-\varphi_n)}}{M_n\omega_n^2\left[\sqrt{(1-\bar{\omega}_n^2)+(2\zeta_n\bar{\omega}_n)^2}\right]}=$$

$$\sum_{n=1}^{\infty}A_nB_n\phi_n(x,y)\mathrm{e}^{\mathrm{i}(\omega t-\varphi_n)}=$$

$$\sum_{n=1}^{\infty}q_n(t)\phi_n(x,y) \tag{9}$$

where the correlation coefficients in the formula have the following form

$$\begin{cases}A_n=\dfrac{F_0\phi_n(x_0,y_0)}{M_n\omega_n^2}\\ B_n=\dfrac{1}{\left[\sqrt{(1-\bar{\omega}_n^2)+(2\zeta_n\bar{\omega}_n)^2}\right]}\\ q_n(t)=A_nB_n\mathrm{e}^{\mathrm{i}(\omega t-\varphi_n)}\end{cases} \tag{10}$$

According to the relationship between interface shear stress and mechanical power in Ref.[20], the corresponding mechanical power of the overall vibration structure to generate the interface shear stress can be expressed as the function of excitation force and the velocity of elements

$$P_n=\frac{1}{2}F_nv_n \tag{11}$$

Combining Eq.(11) and the modal force expression function in Eq.(10), one can get the mechanical power expression, which is shown below

$$P_n=\frac{1}{2}F_nv_n=\frac{1}{2}F_n\dot{w}(x,y,t)=$$

$$\frac{1}{2}F_n\dot{q}_n(t)\phi_n(x,y)=$$

$$\frac{1}{2}F_n\dot{q}_n(t)\phi_n(x,y)=$$

$$\frac{1}{2}\frac{F_0^2\phi_n^2(x_0,y_0)\omega\mathrm{e}^{\mathrm{i}(2\omega t-\varphi)}\phi_n(x,y)}{M_n\omega_n^2\sqrt{(1-\bar{\omega}_n^2)+(2\zeta_n\bar{\omega}_n)^2}} \tag{12}$$

Based on the numerical results of interface shear stress in Ref.[6], the ratio between interface shear stress and the square root of mechanical power is constant for a specific vibration mode, so the interface shear stress can be expressed as

$$\tau_{\text{interface}}=R_{\text{C}}\cdot\sqrt{P_n}=$$

$$R_{\text{C}}\cdot\sqrt{\frac{F_0^2\phi_n^2(x_0,y_0)\omega\mathrm{e}^{\mathrm{i}(2\omega t-\varphi)}\phi_n(x,y)}{2M_n\omega_n^2\sqrt{(1-\bar{\omega}_n^2)+(2\zeta_n\bar{\omega}_n)^2}}}=$$

$$\phi_n(x_0,y_0)\sqrt{\phi_n(x,y)}\cdot\cdots\cdot$$

$$\sqrt{\frac{F_0R_{\text{C}}^2\omega\mathrm{e}^{\mathrm{i}(2\omega t-\varphi)}}{2M_n\omega_n^2\sqrt{(1-\bar{\omega}_n^2)+(2\zeta_n\bar{\omega}_n)^2}}} \tag{13}$$

where R_{C} is the constant ratio value between interface shear stress and the square root of mechanical power. It can be concluded from the above equation that interface shear stress is proportional to the vibration mode characteristics in a specific vibration frequency, and the relationship can be given as

$$\tau_{\text{interface}}\propto\phi_n(x_0,y_0)\sqrt{\phi_n(x,y)} \tag{14}$$

The normalized displacement modes of the thin plate structure can be written in the form of a trigonometric function expression $\phi_n(x,y)=\sin(m\pi x/a)\sin(n\pi y/b)$. The interface shear stress in Eq.(14) can also be written as

$$\tau_{\text{interface}}\propto\phi_n(x_0,y_0)\sqrt{\phi_n(x,y)}=$$

$$\sin\frac{m\pi x_0}{a}\sin\frac{n\pi y_0}{b}\sqrt{\sin\frac{m\pi x}{a}\sin\frac{n\pi y}{b}} \tag{15}$$

From the equation above, a relationship is established between interface shear stress and the normalized characteristics of displacement modes, under the influence of a concentrated excitation force.

2 Methods and Experiment Setups

2.1 Simulation model

A three-dimensional finite element model (FEM) of an aluminum plate with an ice layer attached to its surface is used to simulate the stress-strain level of the whole structure. The dimensions of the plate and ice are 300 mm×100 mm×1 mm and 298 mm×98 mm×1 mm, separately. To avoid fixing the edge of the ice layer when applying clamped boundary constraints, the ice layer size will be slightly smaller than the plate size. According to the research results on size independence of the finite element mesh for de-icing simulation in Ref.[21], the mesh size of 0.001 m was selected to build FEM in this paper. The 8-node quadrilateral element Solid 185 for solid materials was chosen as the basic finite element type to model the thin plate and ice layer. Material information of the plate and ice layer is shown in Table 1.

Table 1 Material parameters of ice and aluminum

Material parameter	Aluminum	Ice
Density/(kg•m^{-3})	2 780	919.7
Young's modulus/GPa	70.5	9.33
Poisson's ratio	0.33	0.325

Four edges of a thin plate were applied to the clamped boundary conditions to guarantee the clear identification of flexural vibration modes. The single excitation force along the Z-direction was applied on the central node of the thin plate. Detailed FEM and some specific monitor points are shown in Fig.1.

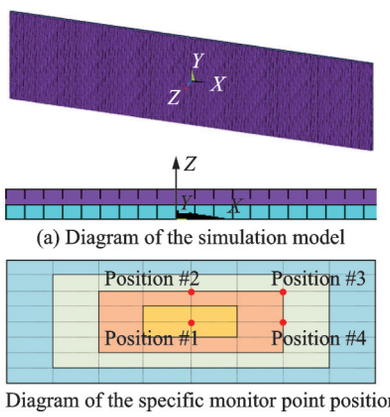

Fig.1 Diagram of the simulation model and specific monitor point positions

2.2 Batch simulation process

The traditional simulation process during harmonic analysis in the commercial FEM simulation software Ansys® uses the combination of frequency range and segmented values to determine the detailed simulation frequencies. However, the natural frequencies of structure do always not fit these frequency settings. So to simulate the deformation and stress response at each natural frequency, a new simulation process was designed through the secondary development method of finite element simulation software. Natural frequencies of this coupled model from 0 to 70 kHz, obtained through modal analysis, are treated as the input for structure deformation and stress simulation. A fixed value exciting force 1 N is applied to the coupled structure during harmonic analysis simulation. Shear stress distribution along with all frequency ranges (0—70 kHz) and detail mode shape information will be obtained to conduct the final analysis. Due to the large simulation cases, the batch calculation method is adopted using the commercial software combination of Matlab® and Ansys®. The main simulation program developed in this work is composed of the union calling of different software, FEM simulation, and data output, in which three parts are run integrally during the calculation.

2.3 Experiment setups

For the actual de-icing experiments conducted in this paper, the piezoelectric actuators were selected as the excitation source to motivate the thin plate. To verify the relationships between interface shear stress and the vibration mode characteristics, the detailed vibration mode shapes during the de-icing process should be checked. So the experiment setups were divided into two aspects: (1) Experiment setup to measure the vibration mode shape, and (2) experiment setup to conduct the final de-icing process. As shown in Fig.2(a), a PSV-500-3D scanning laser vibrometer was used to measure the vibration mode shapes using the laser Doppler principle. The de-icing process was carried out by the setups including the icing environment, camera recording equipment, and the main de-icing structures. An excitation system including a signal generator and power amplifier was used to motivate the piezoelectric actuators during the tests. For better ice removal results that can be observed during the de-icing test, a matching inductance was used to connect in series in the system to improve the final load power for de-icing.

According to the de-icing tests described in much of the literature, when the de-icing test is carried out for a wide range of ice layers, ice cracks always appear inside the ice layer. Therefore, in order to fully verify the contribution of shear stress to de-icing and to obtain a clear ice detachment phenomenon, a special type of ice cube has been designed to ensure a small interface area with the substrate. For the actual inflight de-icing situation to form mixed ice or rim ice under −10 ℃, the supercooled droplets or ice crystals will quickly freeze on the surface of the wing, forming a small contact area with the

wing[1-2]. So the icing model set in this paper is in line with the actual inflight icing cases and also in line with the research in Ref.[22]. As shown in Fig.2(b), the small ice cubes have a spherical shape and have a small contact surface with the thin plate. The effect of interface shear stress for ice delamination will become more obvious while avoiding the ice cracks inside the ice cubes. The ice cubes were made using pure water inside the refrigerator with an icing temperature of −20 ℃. The frozen time was been controlled by around 10 min to guarantee complete freezing. The de-icing test was conducted after finishing the icing process.

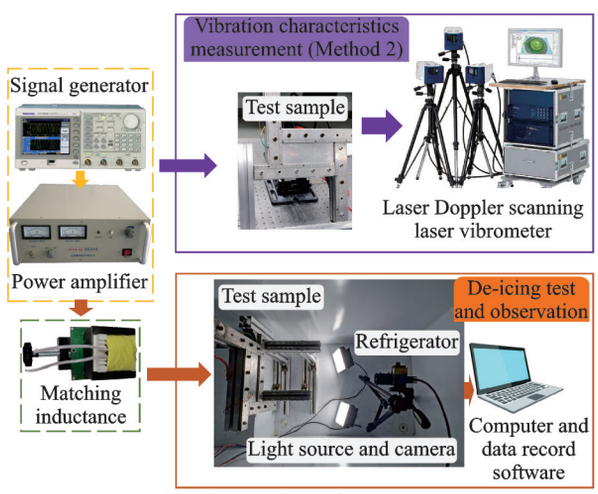

(a) Diagram of experiment setups

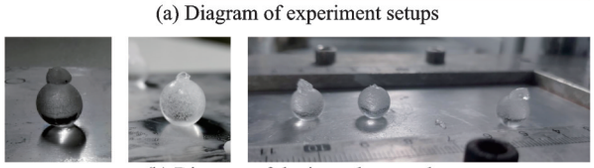

(b) Diagram of the ice cube samples

Fig.2 Diagram of the experimental setups and ice cube samples

3 Results and Discussion

3.1 Distribution characteristics of related vibration parameters with different vibration modes

Some typical vibration parameters, such as displacement, mechanical strain, and mechanical stress, are all related parameters to judge the strength of structure vibration. And the vibration strength of the structure can affect the final ice removal results. So many scholars tried to improve the vibration intensity using different design methods in Refs.[5-15]. Among these design methods, the vibration modes corresponding to different natural vibration frequencies were one of the important aspects to be considered. Fig.3 shows the associated vibration parameter results at the center point of the thin plate with different vibration eigen frequencies. Four types of parameters were outputted from the simulation process. From Fig.3, we can find that the related displacement, stress, and strain all have the same changing trends with vibration frequencies. Some relative maximum points can be identified in these four different trends where parameters are varied. When comparing the interface shear stress with the other three parameters, it can be seen that all three parameters show the vibration frequency points with the relative maximum value of interface shear stress in the low-frequency range. However, only total mechanical equivalent strain and stress can identify these particular frequency points in the high-frequency range. That means the displacement cannot extract all the typical characteristic frequency values, especially in the high-frequency excitation range. Meanwhile, the result also shows that the large displacement represents the large vibration intensity of the structure, but it does not represent the strong shear stress. Therefore, ensuring the vibra-

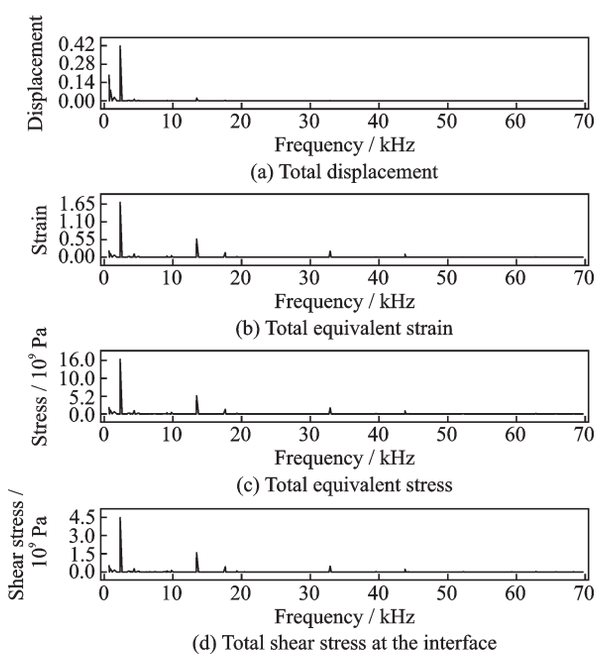

Fig.3 Related vibration parameters in the central point of the thin plate

tion intensity of the structure is the basic condition to ensure de-icing. To finally achieve the de-icing effect, more detailed designs and regulations are needed on this basis.

3.2 Distribution characteristics of interface shear stress with different vibration modes

The total shear stress at the interface between two different substances with a frequency range from 0 to 70 kHz is shown in Fig.4. It shows that shear stress at low frequencies is greater than that at high frequencies, and several much larger points are all in the low-frequency region (< 20 kHz). This is because, under the same external excitation force, the amount of deformation of the coupled structure under low-frequency vibration is greater than that under high-frequency vibration. However, because of the low quantity of antinodes at low frequencies, except in select locations where sufficient shear stress can develop for de-icing, the shear stress produced in other areas with minimal deformation is inadequate for de-icing. For high-frequency vibration, sufficient shear stress can be generated in many areas for ice delamination due to the larger number of anti-nodes while ensuring sufficient excitation capacity. It is also shown in Fig.4 that many maximum points with closing frequency values appear in much higher frequencies (45—70 kHz). So when performing structure de-icing under high-frequency excitation vibration, multiple adjacent usable frequency points are beneficial to the frequency modulation of the whole de-icing system to achieve the best ice-removing effect. In other words, the sweep frequency excitation de-icing method can be used in a high-frequency range to obtain better de-icing results.

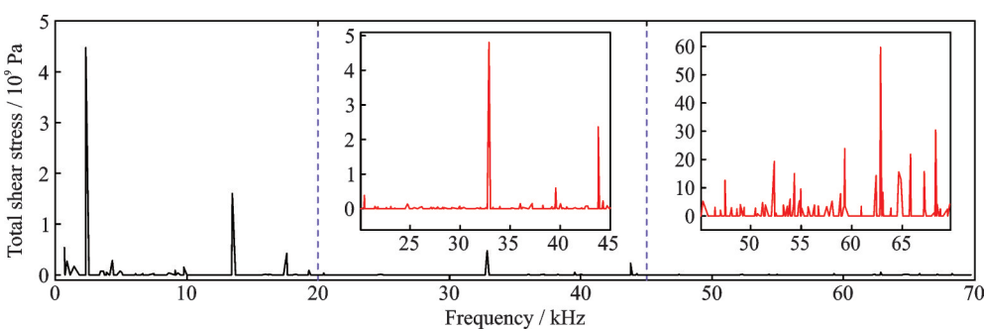

Fig.4 Total shear stress at the interface with the frequency range from 0 to 70 kHz

3.3 Distribution characteristics of the optimal de-icing modes corresponding to different positions

Results of the top 10 interface shear stress values and corresponding natural frequencies at different monitoring positions are shown in Fig.5. The excitation frequency of the extreme point of the interface shear stress can produce a better de-icing effect in many positions of the structure. That means, for some specific vibration modes, the de-icing effect can be achieved in a larger area (e.g. vibration mode of 2 309.4, 13 455, 32 894, and 17 630 Hz). These optimal de-icing modes can be treated as the target de-icing modes for the ice removal process with single vibration mode excitation. That's also the common way adopted in many literatures to conduct the de-icing test due to the convenience of the excitation operation. Because the actual vibration modes of the structure at its natural frequency may not be very regular due to errors in manufacturing and fixing, selecting a single vibration mode excitation method at one optimal de-icing mode may not fulfill the final de-icing requirement. So trying to change the vibration mode shapes when conducting the de-icing excitation will be a convenient method. For example, in the de-icing process of every single point, the de-icing purpose is realized by reciprocating excitation according to the frequencies corresponding to the top 10 interface shear stresses. That's also another type of sweep frequency excitation de-icing method that can be used in the de-icing application.

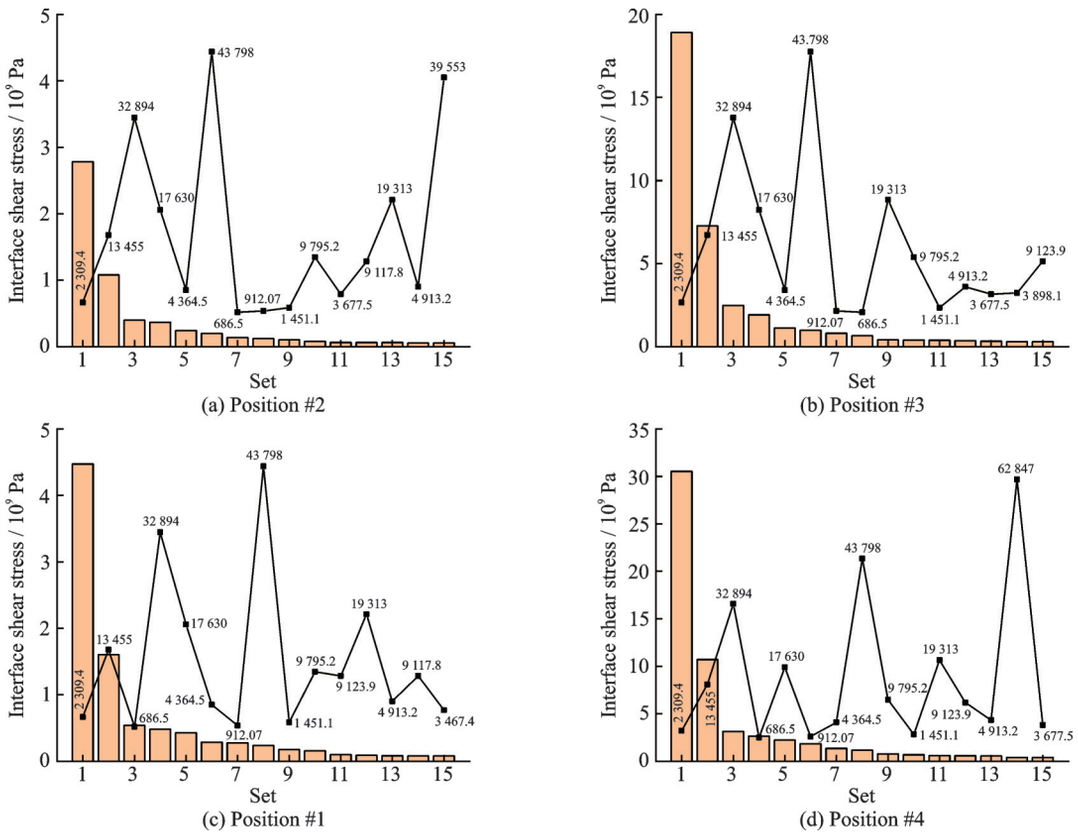

Fig.5 Top 10 interface shear stress values and corresponding frequencies at different positions

3.4 Corresponding relationship between modal parameters and de-icing shear stress

A comparison of mode shapes information and total shear stress is shown in Fig.6. Structure mode shape information is described by the value m and n, while m is the number of anti-nodes in the transversal axis and n is considered as the number of anti-nodes in the longitudinal axis[18]. These two parameters also are called the number of anti-nodes in different directions. The maximum shear stress almost appears when m and n are odd, which means that when the structure is driven to have a symmetrical mode shape, it has a better de-icing effect than an anti-symmetric mode. According to Eq.(15), the expression of interface shear stress at the central point of the thin plate $(x_0, y_0)=(x, y)=(a/2, b/2)$ can be written as

$$\tau_{\text{interface}} \propto \phi_n(x_0, y_0)\sqrt{\phi_n(x, y)} = \sin\frac{m\pi}{2}\sin\frac{n\pi}{2}\sqrt{\sin\frac{m\pi}{2}\sin\frac{n\pi}{2}} \tag{16}$$

It can be concluded from Eq.(16) that if m and n are odd, the interface shear stress will be the maximum value (equal to 1). That's also consistent with the simulation results shown in Fig.6. From the perspective of vibration mode shapes, the maximum value of interface shear stress will appear at the anti-nodes position of vibration modes. When the excitation force is located at the central point of the thin plate, the highest value will be achieved if the product of the target de-icing position's coordinate and the anti-node numbers are nearly odd. The shear stress equation presented in this paper can be employed to estimate the shear stress at various positions on the thin plate that exhibit flexural vibration modes.

The relationship between other vibration mode characteristics ($m\times n$) and interface shear stress is shown in Fig.7. Vibration frequencies corresponding to the top 30 interface shear stress values were selected and compared in the figure. The read small diamond blocks represent the frequencies corresponding to the top 17 interface shear stress values. Fig.7 shows that when the value of $m\times n$ is odd (that means the vibration mode with its parameters is a symmetrical mode), the interface shear stress exhibits a higher level. This is also consistent with the results in Fig.6. And when studying the changing

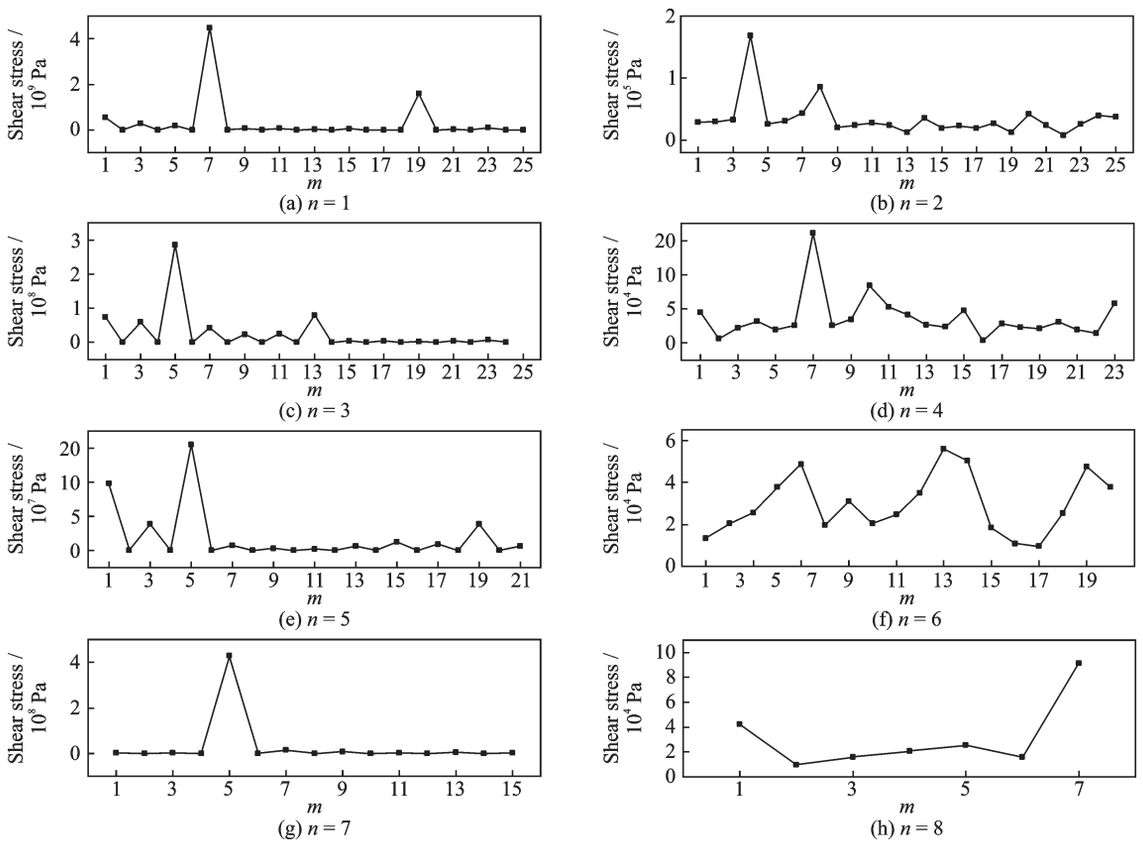

Fig.6 Comparison of mode shape information and total shear stress

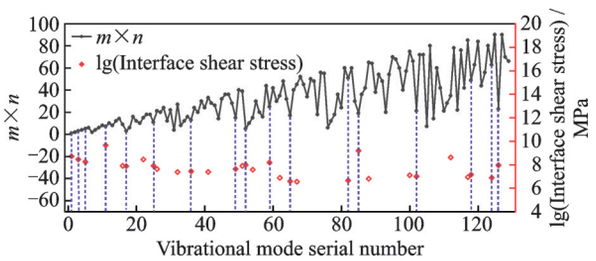

Fig.7 Comparison results of vibration mode parameters $m\times n$ and interface shear stress

trend of $m\times n$ value, it can be found that in the region of local frequency variation, the corresponding structural mode is easy to obtain a higher shear stress level when $m\times n$ has a minimum value.

3.5 Verification of simulation method and de-icing experiment results

The verification of simulation results and experiment results was conducted according to the measurement data and the related calculation data. To verify the applicability of the conclusions of the study on different structures, a thin plate with a size of 160 mm×80 mm×2 mm was used to verify the de-icing results under different vibration mode characteristics. The main aspects to be compared are vibration mode shapes and relative vibration frequencies. As discussed in Section 2.1, the piezo-actuator was chosen as the excitation source to vibrate the plate. So the verification of the simulation method and the de-icing experiments were conducted using the thin plate with a piezo-actuator. Comparison results of vibration frequencies and typical vibration mode shapes are shown in Fig.8 and Fig.9, separately. The correspondence between the simulation outcomes and the measurement outcomes of vibration frequencies and linked vibration mode shapes confirms the accuracy of the finite element simulation technique.

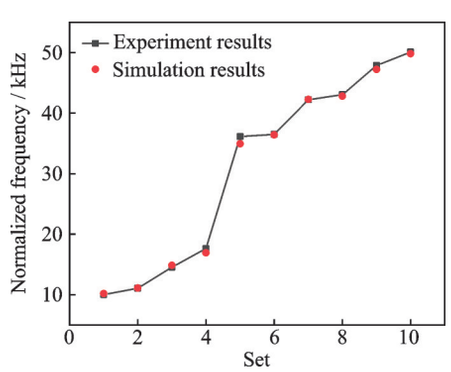

Fig.8 Comparison results of vibration frequencies

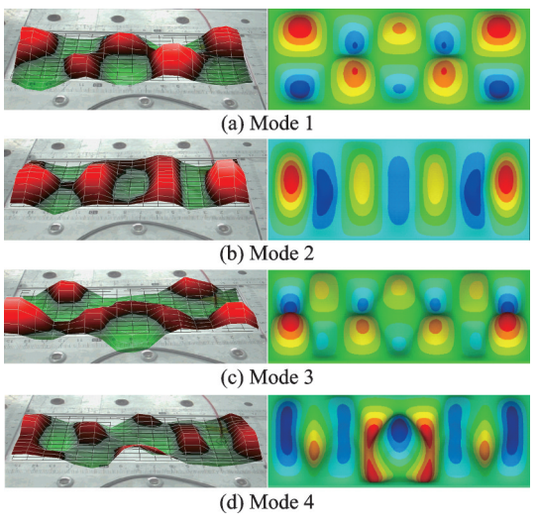

Fig.9 Comparison results of typical vibration mode shapes

Three different flexural vibration modes of the thin plate were selected as the de-icing vibration frequencies in the ice removal experiments. The central point of the thin plate was treated as the target de-icing position and bonded with the ice cubes. The de-icing experiments were conducted in the refrigerator with the icing temperature of −20 ℃, and the de-icing results were observed and recorded by a low temperature resistant industrial camera and its light source system. So the de-icing time of each case will be recorded and analyzed through these experiment videos. By adjusting the series matching inductance, the load power of each de-icing test was stabilized at 12.5 W to guarantee equal input excitation power. Because the excitation source employed piezoelectric ceramic rather than standard single-point excitation force, the de-icing verification experiments just aimed to confirm the outcomes of flexural vibration modes with different m and n combinations in this article. Fig.10 shows the de-icing results under three different flexural vibration modes. It can be found that the vibration mode with the combination of "m=11 & n=3" has a larger interface shear stress to induce the ice delamination results than the other two vibration modes. So the vibration mode with odd m and odd n values has the better de-icing effect. The target de-icing flexural vibration mode can be selected initially based on the characteristics of m and n values.

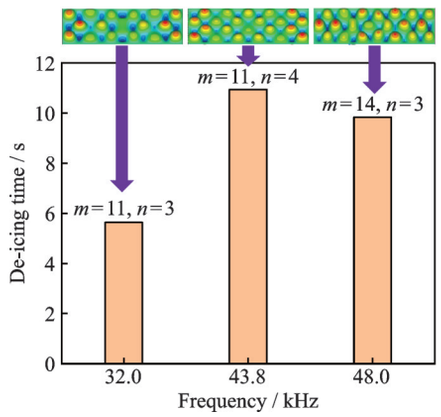

Fig.10 De-icing results on the thin plate under three different flexural vibration modes

4 Conclusions

The distribution characteristics of de-icing shear stress and related vibration parameters on the thin plate were discussed based on the simulation method and theoretical derivation. The study established the relationship between interface shear stress and vibration mode characteristics of a thin plate under a single excitation force through theoretical derivation. The simulation method with batch calculation process revealed varying parameter distribution outcomes related to ice removal. Final experiments on vibration dynamic features measurements and de-icing attempts implemented the verification of the simulation method and results found in this research. The conclusions discovered in this paper are summarized below:

(1) The connection of shear stress and vibration mode feature was derived by the theoretical method on a thin plate. The shear stress induced on a thin plate's interface by a single force's excitation is directly proportional to the vibration mode characteristics at a certain frequency of vibration and as a function of normalized displacement modes. This correlation depends on the coordinates of the force and de-icing positions.

(2) Characteristic frequencies with maximum interface shear stress values can be distinguished through the changing curves of displacement, total mechanical equivalent stress, and strain in the low-frequency range, while these frequencies in the high-frequency range only can be separated through total

equivalent stress and strain.

(3) Low-frequency range will appear large interface shear stress for single-frequency excitation, and the high-frequency range will guarantee the sweep frequency excitation for de-icing. Meanwhile, de-icing outcomes can be achieved from various locations by selecting particular frequencies for individual or sweeping excitation.

(4) Maximum interface shear stress will be induced on the thin plate under the flexural vibration modes with odd m and odd n values. At the same time, for de-icing at the central position of the plate, the symmetrical mode shape is beneficial for inducing ice removal. De-icing results with three different frequencies under the temperature of −20 ℃ were conducted. Successful ice delamination results and comparison with vibration mode characteristics also verified the conclusions researched in this paper. Initial de-icing mode selection based on the characteristics of m and n values of the flexural vibration modes can be used in the mechanical vibration de-icing system design.

References

[1] ZEPPETELLI D, HABASHI W G. In-flight icing risk management through computational fluid dynamics-icing analysis[J]. Journal of Aircraft, 2012, 49(2): 611-621.

[2] FENG K, LU Z, YUN W. Aircraft icing severity analysis considering three uncertainty types[J]. AIAA Journal, 2019, 57(4): 1514-1522.

[3] PEI B, XU H, XUE Y. Flight-safety space and cause of incident under icing conditions[J]. Journal of Guidance, Control, and Dynamics, 2017, 40(11): 2983-2990.

[4] WANG Y, XU Y, HUANG Q. Progress on ultrasonic guided waves de-icing techniques in improving aviation energy efficiency[J]. Renewable and Sustainable Energy Reviews, 2017, 79: 638-645.

[5] VENNA S V, LIN Y J, BOTURA G. Piezoelectric transducer actuated leading edge de-icing with simultaneous shear and impulse forces[J]. Journal of Aircraft, 2007, 44(2): 509-515.

[6] PALACIOS J, SMITH E, ROSE J. Investigation of an ultrasonic ice protection system for helicopter rotor blades[J]. Annual Forum Proceedings of American Helicopter Society, 2008, 64(1): 609.

[7] PALACIOS J, SMITH E, ROSE J, et al. Ultrasonic de-icing of wind-tunnel impact icing[J]. Journal of Aircraft, 2011, 48(3): 1020-1027.

[8] KALKOWSKI M K, WATERS T P, RUSTIGHI E. Removing surface accretions with piezo-excited high-frequency structural waves[C]//Proceedings of Active and Passive Smart Structures and Integrated Systems 2015. [S.l.]: SPIE, 2015, 9431: 504-518.

[9] KALKOWSKI M K, WATERS T P, RUSTIGHI E. Delamination of surface accretions with structural waves: Piezo-actuation and power requirements[J]. Journal of Intelligent Material Systems and Structures, 2017, 28(11): 1454-1471.

[10] HABIBI H, CHENG L, ZHENG H, et al. A dual de-icing system for wind turbine blades combining high-power ultrasonic guided waves and low-frequency forced vibrations[J]. Renewable Energy, 2015, 83: 859-870.

[11] TAN H, ZHANG X, ZHANG L, et al. Ultrasonic influence mechanism of a cold surface frosting process and an optimized defrosting technique[J]. Applied Thermal Engineering, 2019, 153: 113-127.

[12] GUO F, WU J H. Mechanism and prediction models for interfacial shear separation of claddings excited by Love waves[J]. Advances in Mechanical Engineering, 2021, 13(3): 16878140211005196.

[13] VILLENEUVE E, GHINET S, VOLAT C. Experimental study of a piezoelectric de-icing system implemented to rotorcraft blades[J]. Applied Sciences, 2021, 11(21): 9869.

[14] BUDINGER M, POMMIER-BUDINGER V, BENNANI L, et al. Electromechanical resonant ice protection systems: Analysis of fracture propagation mechanisms[J]. AIAA Journal, 2018, 56(11): 4412-4422.

[15] BUDINGER M, POMMIER-BUDINGER V, REYSSET A, et al. Electromechanical resonant ice protection systems: Energetic and power considerations[J]. AIAA Journal, 2021, 59(7): 2590-2602.

[16] PALANQUE V, MARBŒUF A, BUDINGER M, et al. Improving mechanical ice protection systems with substrate shape optimization[J]. Cold Regions Science and Technology, 2022, 202: 103641.

[17] ROUSET P, BUDINGER M, BUDINGER V. Comparison of extensional and flexural modes for the design of piezoelectric ice protection systems[C]//Proceedings of EUCASS 2017. Milano, Italy: [s.n.], 2017.

[18] ZHAO C. Ultrasonic motors: Technologies and applications[M]. [S.l.]: Springer Science & Business Media, 2011.

[19] WANG C Y, WANG C M. Structural vibration: Exact solutions for strings, membranes, beams, and plates[M]. Calabasas, USA: CRC Press, 2013.

[20] POMMIER-BUDINGER V, BUDINGER M, TEPYLO N, et al. Analysis of piezoelectric ice protection systems combined with ice-phobic coatings[C]// Proceedings of the 8th AIAA Atmospheric and Space Environments Conference. USA: AIAA, 2016: 3442.

[21] GUO W, DONG X, LI Y, et al. Simulations on vibration mode and distribution of shear stress for icing aluminum plate excited by ultrasonic vibration[J]. Advances in Mechanical Engineering, 2020, 12(3): 1687814020911231.

[22] ZENG X C, YAN Z X, LU Y C, et al. Reduction of Ice adhesion using surface acoustic waves: Nanoscale vibration and interface heating effects[J]. Langmuir, 2021, 37(40): 11851-11858.

Acknowledgements This work was funded by the National Natural Science Foundation of China (Nos.11832012, 12227802) and the Fundamental Research Funds for the Central Universities (No.3082020NP2020402). The authors gratefully acknowledge the support of the State Key Laboratory of Mechanics and Control for Aerospace Structures, Nanjing University of Aeronautics and Astronautics because many of the vibration mode measurements presented in this paper were performed in this lab.

Authors Mr. **MIAO Bo** received the B.E. degree in human-machine and environmental engineering and the M.S. degree in aeronautical engineering from Nanjing University of Aeronautics and Astronautics, China, in 2013 and 2016, respectively. He is currently pursuing the Ph.D. degree in human-machine and environmental engineering with Nanjing University of Aeronautics and Astronautics, Nanjing, China. His current research interests include aircraft de-icing systems, ultrasonic actuator design, and coupling de-icing theory.

Prof. **ZHU Chunling** graduated from Nanjing University of Aeronautics and Astronautics, China, in 1990 and completed her M.S. and Ph.D. degrees in Environmental Engineering of Flight Vehicle from Beihang University, China, in 1993, and Nanjing University of Aeronautics and Astronautics, China, in 2007, respectively. Now she leads a research group working on aircraft anti-icing and de-icing problems. Her research interests include aircraft icing mechanisms, icing numerical simulation, and anti/de-icing methods.

Author contributions Mr. **MIAO Bo** designed the study, complied the models, conducted the analysis, interpreted the results, and wrote the manuscript. Mr. **YUAN Lang** contributed data and conducted experiments. Prof. **ZHU Chunling** contributed to the discussion and background of the study and supervised the work. All authors commented on the manuscript draft and approved the submission.

Competing interests The authors declare no competing interests.

(Production Editor: ZHANG Huangqun)

面外弯曲振动薄板上的除冰剪切应力分布特征研究

苗 波[1], 袁 浪[1], 朱春玲[2]

(1.南京航空航天大学航空学院,南京 210016,中国;
2.南京航空航天大学航空航天结构力学与控制国家重点实验室,南京 210016,中国)

摘要:基于压电驱动器激励振动的机械力学式除冰技术是一种重量小和能耗低的新型除冰技术,用于应对航空结冰威胁问题。其中机械振动引起的界面剪切应力和相应结构振动模态是该除冰技术研究中的两个重要方面。寻找合适的振动模态来产生足够的界面剪切应力以提高除冰效率是研究中的重要内容。薄板的振动模态通常用横向轴线和纵向轴线上的反节点数m和n来描述。本文目的是研究不同结构弯曲振动模态下除冰剪切应力的分布特征,从而为基于机械振动的结冰防护系统(Ice protection system, IPS)的详细设计建立目标振动模态的选择依据。通过理论分析和仿真计算,建立了界面剪切应力与结构振动模态参数之间的关系。采用"冰层-平板-压电陶瓷"的有限元分析模型(Finite element model, FEM),仿真计算了不同振动模态下的应力应变水平,并根据仿真和实验结果分析了除冰剪切力的分布特征。最终给出了基于弯曲振动模态参数m和n的特征来确定除冰模态的选择标准。

关键词:除冰方法;界面剪切应力;振动模态;分布特征;有限元模型;结冰防护系统